

Journal of the Electrochemical Society, Vol. 146, No. 10, 1999, pp. 3672-3678.

ISSN: 0013-4651

DOI: 10.1149/1.1392532

<http://scitation.aip.org/getpdf/servlet/GetPDFServlet?filetype=pdf&id=JES0AN000146000010003672000001&idtype=cvips&prog=normal>

<http://www.electrochem.org/>

© The Electrochemical Society, Inc. 1999. All rights reserved. Except as provided under U.S. copyright law, this work may not be reproduced, resold, distributed, or modified without the express permission of The Electrochemical Society (ECS). The archival version of this work was published in Journal of the Electrochemical Society, Vol. 146, No. 10, 1999, pp. 3672-3678.

Oxidation of Zr-2.5 Nb Nuclear Reactor Pressure Tubes A New Model

A. J. Markworth, A. Sehgal,* and G. S. Frankel**

Fontana Corrosion Center, Department of Materials Science and Engineering, The Ohio State University, Columbus, Ohio

** Electrochemical Society Student Member. * Electrochemical Society Active Member.

The corrosion and associated deuterium (D) uptake of Zr alloy nuclear reactor pressure tubes have been studied for over 40 years. Zircaloy tubes exhibit rapid D ingress after a period of in-reactor exposure, and have been replaced with tubes fabricated from the more resistant Zr-2.5 wt % Nb alloy. Recently, however, a small percentage of Zr-2.5 Nb tubes have been found to contain high D contents. There is currently no clear understanding of the mechanism for this increased D uptake, and concern exists that an increasing number of high-D tubes will develop with time. A new model for Zr-2.5 Nb corrosion is presented in this paper. The rate of corrosion is shown to be dependent on the rate of transformation of the protective inner oxide layer (closer to the metal) to a porous outer layer. The mechanism of this transformation is not known and should be the subject of future investigations. It is assumed in the model that zirconia chemically dissolves into the solution at the pore bottom. The rate of this dissolution reaction depends on the local pH, which increases if there is a buildup of deuteroyl ions generated in the cathodic part of the Zr corrosion reaction. A mathematical description of this model, containing several parameters with unknown values, is presented. Assigning certain values to these parameters results in predictions of oxide formation (and thus D buildup) that correspond well with observations.

The elevated-temperature aqueous corrosion of zirconium alloys (Zircaloy family and Zr-2.5 wt % Nb) in nuclear reactor environments has been investigated extensively during the past forty years. These materials have been used, for instance, as pressure tubes in CANDU reactors. Zr alloys corrode in the heavy water that is contained by the pressure tubes. The water in the tube has a temperature range of 250-310°C, and the pH is 10.3 as a result of the addition of LiOH.^{1,2} As described in detail in the following discussion, deuterium is evolved during the corrosion process, and about 5-10% of the evolved deuterium is absorbed into the Zr-2.5 Nb alloy.³ Increased D content in Zr-based pressure tubes has resulted in precipitation of zirconium deuterides, blister formation, and subsequent cracking.^{4,5} Since deuterium is an isotope of hydrogen and acts like H when absorbed into metals, this is often referred to as hydrogen uptake and hydride formation.

During the initial years of exposure to the reactor environment, the Zr alloys exhibit a rather constant and low rate of corrosion and hydrogen uptake.^{2,6,7} Figure 1 shows that Zircaloy-2 tubes start to corrode at a faster rate after a period of about five effective full power years (EFPYs), as evidenced by the rate of change of oxide thickness on the tubes and the amount of D in the tubes.⁵ It has been proposed that when the oxide is thin, coolant-borne H₂ can penetrate the oxide to suppress the oxidizing species formed in the oxide pores by radiolysis.⁶ This suppression cannot occur when the oxide reaches a critical thickness of 15-20 μm (larger than

the deuterium penetration range), resulting in an increase in the oxidizing power of the electrolyte in the pores and an increase in the rate of corrosion.⁶ One criticism of this explanation for increased corrosion rates with time is that after a certain oxide thickness is reached and a porous oxide layer (post-transition oxide) forms, deuterium is plentiful and present in the bottom of all pores, provided less than 100% of the deuterium evolved during the cathodic reaction is absorbed by the metal.⁴ Whatever the explanation of this acceleration in Zircalloys, Zr-2.5% Nb tubes do not exhibit this phenomenon to the same extent. Also, the second phase particles present in Zircalloys, but not in Zr-2.5% Nb, have been blamed for this acceleration of attack because they apparently act as preferred sites for D evolution and pickup. As a result, the Zircaloy-2 pressure tubes in CANDU reactors have been replaced with Zr-2.5% Nb.

Zr-2.5% Nb tubes have now been in service for over 14 EFPYs. Most of these tubes have exhibited a constant low rate of corrosion and D uptake over that time.⁸ An empirical model describing the deuterium content in Zr alloy pressure tubes has been presented.² The D concentration, $[D]$, is predicted by this model to increase linearly with time, t , and have an Arrhenius-type dependence on temperature, T

$$[D] = At \exp(-Q/kT) \quad [1]$$

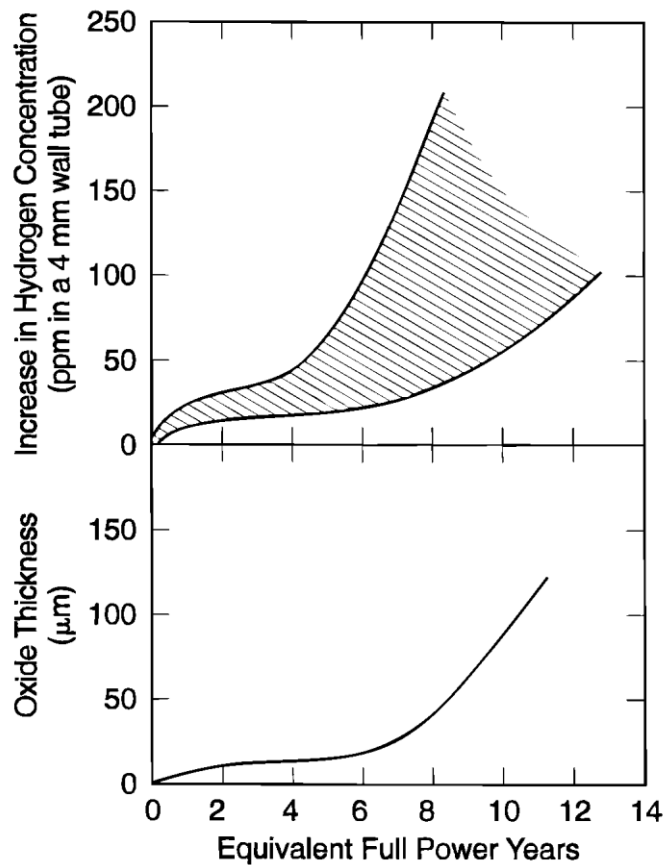


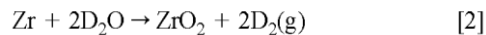
Figure 1. The corrosion and hydrogen increase in Zircaloy-2 pressure tubes after reactor service (from Ref. 5).

where A is a constant, Q is the activation energy for deuterium diffusion through the barrier oxide layer, and k is Boltzmann's constant. The D content will increase linearly with time if the rate of uptake is constant. This indicates, however, that the oxide film is not protective and might be susceptible to spalling and accelerated rates of attack. A protective film would result in a continual decrease in the reaction rate, such as seen in parabolic kinetics.

In fact, there have been a few Zr-2.5 Nb tubes that have exhibited rather high D contents after 8-14 EFPYs, as seen in Fig. 2.² A few anomalously high values explain the scatter shown in Fig. 2. A good explanation for why this small percentage of Zr-2.5 Nb tubes exhibits high D contents has not yet been provided. It has been suggested that this phenomenon results from a loss in control of the composition of the annulus gas that surrounds the outside of the tubes in CANDU reactors.² All the high-D-content tubes had nitrogen gas in the annuli that resulted in a reducing atmosphere on the outside of the tube. It is possible that this leads to oxide degradation on the outside of the tube and hence, increased D uptake. In fact, D uptake in Zr-2.5% Nb has been shown to depend on the exact gas chemistry.¹ However, this phenomenon has not been conclusively proven to explain the existence of the high-D tubes.

Deconvolution of the depth distribution of ¹²C and ¹³C isotopes in both high-D and low-D Zr-2.5% Nb pressure tubes has provided evidence that the rate of oxide growth on the inner surface of high-D tubes increased by a factor of 2-3 after about 9 EFPYs.⁸ The reason for this increase or why only a few tubes exhibit this behavior has not been determined. The observation of these high-D tubes has generated concern that Zr-2.5% Nb is generally susceptible to an acceleration in corrosion and D uptake similar to Zircaloy-2. Some aspects of these processes are reviewed in this paper, and a model for Zr corrosion is presented.

Corrosion and D absorption.—Since the inner diameter (i.d.) surface of the pressure tube is exposed to heavy water, and the outer diameter (o.d.) surface of the pressure tube is exposed to a gaseous environment that contains some water vapor, corrosion of the pressure tube is possible at both surfaces. The corrosion reaction can be written as



A small fraction of the deuterium generated on the surface is absorbed into the pressure tube. Reaction 2 looks simple but is actually quite complex. It involves three regions: the metal, the oxide, and the corrosive environment.⁹ Growth of the oxide is believed to involve movement of anion vacancies.^{9,10} The total reaction can be

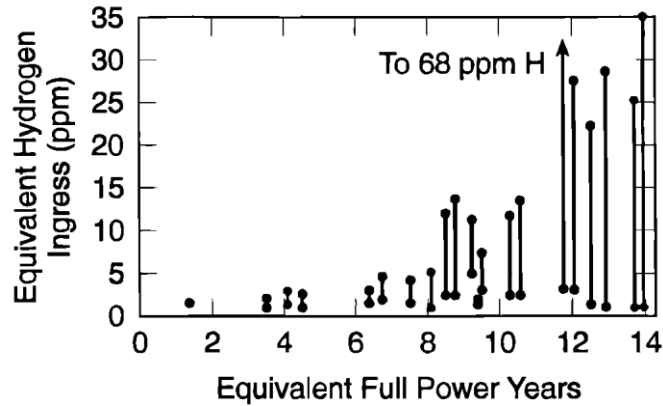
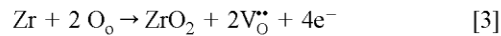
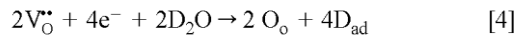


Figure 2. Deuterium contents in pressure tubes removed from Ontario Hydro CANDU reactors (from Ref. 2). It should be noted that data from 9 EFPY and higher were obtained from tubes operated with nitrogen-filled annuli (except for one data point at 9.5 EFPY ranging from 3-8 ppm hydrogen ingress that was obtained with carbon dioxide filled annuli). The more recent data are from CO₂-filled annuli tubes.

divided into an oxidation reaction that occurs at the metal/oxide interface⁹



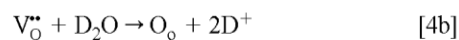
and a reduction reaction that occurs at the oxide/solution interface⁹



where V_o^{••} represents an oxygen ion vacancy in the oxide, O_o is an oxygen ion in the oxide, and D_{ad} is atomic deuterium adsorbed on the oxide surface. It should be noted that these reactions are written in the Kroger-Vink notation, which is commonly used for ionic solids.^{11,12} Reaction 4, in which both water and the oxygen vacancies are reduced, is written with four electrons so that it sums to Eq. 2 when added to Eq. 3 and the following reaction



It has been suggested that D⁺ enters the oxide lattice by⁹



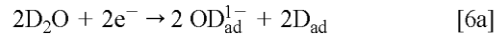
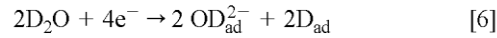
This we consider to be unlikely because it would necessitate movement of a positively charged

species through the oxide film against the potential gradient, which is extremely difficult.

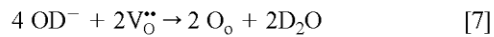
Once formed, the deuterium atoms can recombine to form molecular deuterium and leave the surface as gas (Eq. 4a), or be absorbed into the oxide in the atomic state and diffuse toward the metal/oxide interface (Eq. 5)



It has been shown that the deuterium that diffuses to the base alloy is the reaction product of the Zr corrosion reaction and is not the deuterium gas that is dissolved in the PHT (primary heat transport) coolant.¹³ Infrared spectroscopy has indicated that the dominant D-containing species in the oxide film is a deuteroyl species and not the expected D species.^{1,2} Deuteroyl may form during one of the following reduction reactions



The difference between two reactions is the oxidation state of the D in the deuteroyl species. In reaction 6a the D in the deuteroyl is not reduced, similar to Eq. 4b Note that D is generated along with deuteroyl. Once formed, the deuteroyl species may also then absorb and diffuse into the oxide. Reaction 4 was described as the reduction reaction in the corrosion process. Reaction 6a results in reaction 4 if one considers that the OD^- further reacts with oxygen vacancies



Elmoselhi *et al.*¹ have done some experiments that are at the core of the current understanding of the D transport in zirconium oxides formed on pressure tubes. They studied the D concentration profile following exposure to gaseous atmospheres of predominantly D_2 or D_2O . It was concluded that the D concentration profiles at the inner surface oxide are the sum of two components. Following exposure to D_2O gas, the predominant contribution is from charged deuteroyl groups that are strongly bound to accessible sites along grain boundaries in the i.d. surface oxide. A smaller fraction of the total D in the oxide is due to the mobile deuterium atoms. A sharp D gradient was observed at the oxide-metal interface, with little D actually in the metal. Elmoselhi *et al.* concluded that despite their high concentration in the outer layer of the i.d. oxide, the deuteroyl groups may not be the deuterium-containing species that enters the pressure tube.¹ Deuterium atoms are the most likely deuterium-containing species that enters the pressure tube. The D profile following exposure to D_2 gas was starkly different from D_2O exposure. In this case little D was found in the oxide, whereas the D concentration in the metal

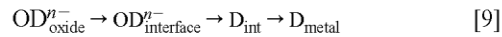
was extremely high. Deuteroyl is apparently associated with water-containing environments.

Interestingly, experiments done by Elmoselhi *et al.*¹ to determine mobility of deuterium in the oxide layer showed quantitatively that deuterium could be replaced by hydrogen and vice versa, in times much shorter than it took to establish the original profile, without changing the original profile. This shows that the deuterium and deuterium-containing species are mobile throughout the oxide when the surface is exposed to D₂O. In spite of these experiments, the diffusing deuterium-containing species and permeation paths have yet to be unequivocally established.

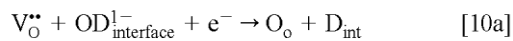
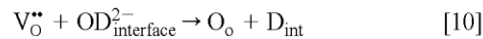
At the oxide/metal interface, the Zr dissolution reaction, Eq. 2, occurs. Other reactions also take place there. Diffusing deuterium enters the metal and may pass through a state at the interface



If deuterium associated with deuteroyl enters the metal, another series of steps must occur



Depending upon the charge of the deuteroyl, the transformation of deuteroyl to D may or may not involve reduction

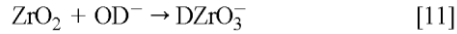


The net result of the possible corrosion reactions described in Eq. 2-10 is the formation of oxide on the Zr tube surface and uptake of D into the tube.

Model for Corrosion of Zr-2.5 Nb Tubes and D Uptake

Model description.—Many mechanistic, semi-empirical and empirical models for Zircaloy corrosion have been presented and critically compared in a recent publication.⁴ Apart from the model presented earlier in the introduction, there is no published model in open literature on Zr-2.5 Nb corrosion. We have assembled a new model to describe the corrosion of Zr-2.5 Nb tubes. In this model, the zirconium oxide layer is treated as a bilayer with an inner protective barrier and an outer porous nonprotective layer. It is assumed that the rate of corrosion depends solely on transport across the dense barrier layer. The point defect model of oxide film

growth of Macdonald *et al.*^{11,12,14,15} has been used to describe this phenomenon. The transformation of the barrier layer into a nonprotective porous layer at the outer side of the barrier layer ultimately controls the reaction, because the thickness of the barrier layer is dependent on this transformation. Similar work has been reported by Macdonald on oxide films in which the steady-state growth and dissolution of the barrier layer was studied.¹⁶ Work done by Pensado-Rodriguez *et al.*^{17,18} on Li oxides in alkaline solutions has clearly shown that at steady state the cathodic reaction in the system, hydrogen evolution, is proportional to the porosity of the outer layer and that porosity is needed to maintain water transport to allow the cathodic process to occur. In Zr-2.5 Nb, the exact mechanism for the transformation of a dense barrier layer to a nonprotective porous layer is not understood but is critical to the entire corrosion reaction. In our model, we assume that this transformation occurs as a result of chemical dissolution of the zirconium oxide. Zirconia will dissolve chemically to form zirconate if the pH is high enough

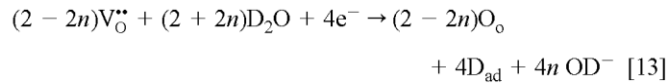


The solubility of the zirconate is pH-dependent and at room temperature is given by¹⁹

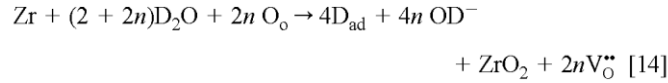
$$[\text{DZrO}_3^-] = 10^{-17.46+\text{pH}} = 10^{-3.46+\log[\text{OD}^-]} \quad [12]$$

This solubility is actually for hydrated oxide, $\text{ZrO}_2\text{-H}_2\text{O}$. As discussed in the earlier section, there is evidence that under some conditions, D in the oxide is present in the form of a deuteroyl. Equations 6 and 6a describe the reactions that might form the deuteroyl, depending upon the oxidation state. If OD^- forms, the pH would certainly increase.

The sum of reactions 6a and 7 is reaction 4. The reduction reaction 4 can thus be viewed as a two-step reaction. It describes the reduction process if all the deuteroyl formed by water reduction reacts further. Under these conditions there will be no increase in pH associated with the cathodic reaction. If, however, not all the deuteroyl generated in reaction 7 reacts further, there can be an increase in pH. This increase would occur at the location of the cathodic reaction, which has been described to be at the oxide/solution interface. Considering, however, that the oxide is a bilayer with the dense inner layer controlling the reaction, it is reasonable to assume that the cathodic reaction occurs at the bottom of the pores, *i.e.*, at the barrier layer/porous layer interface. If there is an increase in pH associated with the cathodic reaction, this would occur at the position where the barrier layer is transformed into porous layer. Therefore, the increase in pH may be responsible for the transformation of the dense barrier layer to a nonprotective porous layer. The cathodic reaction may be generalized to include the possibility of some deuteroyl formation



where n is the fractional amount of reduction associated with deuteroyl formation. Equation 13 reduces to Eq. 4 if $n = 0$ and to reaction 6a if $n = 1$. The total zirconium corrosion reaction is obtained by adding reaction 13 to reaction 3 to get



This reaction reduces to reaction 2 if $n = 0$ and assuming that the adsorbed D recombines to form D_2 . Along with the increase in pH resulting from the generation of OD^- , a consequence of this reaction scheme is that the oxide is nonstoichiometric; there should be excess oxygen vacancies in the oxide.

The consumption of water atoms in the cathodic reaction also effectively results in an increase in pH owing to a concentration of the added LiOH. This effect has not yet been included in the model.

The zirconia dissolution reaction, Eq. 11, consumes deuteroyl, which decreases the pH and slows the dissolution reaction. The excess deuteroyl diffuses, along with the zirconate ions, out of the pores. As the pH decreases along the pore length, the zirconate ion may reprecipitate as zirconia. The rate of dissolution of zirconium metal is controlled by the thickness of the barrier oxide layer, which is being transformed to a barrier layer by chemical dissolution owing to the increase in pH.

This mechanism of dissolution/reprecipitation has been discussed by Cox and Fidleris.²⁰ They found that porosity is developed in ZrO_2 films during irradiation with UV light if a large electric field is present. This behavior was observed in concentrated alkaline and acidic electrolytes where zirconia is relatively soluble. It was suggested, however, that similar reactions could occur in reactor environments and that a dissolution/reprecipitation mechanism was responsible.

Mathematical implementation of the model.—In this section the above-described model is expressed in mathematical form as a set of coupled, nonlinear, ordinary differential equations. Solutions generated numerically, using somewhat arbitrarily selected sets of values for the system parameters, are described in the section that follows.

Let L_b be the thickness of the barrier layer at time t . The first thing we establish is an expression for dL_b/dt , to which there are two contributions. One arises from barrier-film formation at the m/b (metal/barrier) interface. The other is a loss term and results from transformation of dense barrier material to porous material at the b/p interface, which is the assumed sharp boundary between the barrier and the porous layers. For the former, we use the film-growth model of Macdonald and co-workers^{11,12,14,15} and for the latter, the classic dissolution-kinetics formalism for a mineral dissolving into an aqueous medium.²¹ We thus obtain

$$\frac{dL_b}{dt} = \frac{A'(B-1)}{\exp(2KL_b) - 1} - R \quad [15]$$

where

$$R = k_1(C_{ze} - C_z)^j \quad [16]$$

Here A' , B , K , and k_1 are parameters that depend on temperature but not on any of the system variables. Also, C_{ze} and C_z are, respectively, the equilibrium and actual concentration of zirconate ions at the b/p interface in the electrolyte contained within the pores of the porous layer, and j can be any positive number (not necessarily an integer). From Eq. 12, we deduce

$$C_{ze} = \alpha C_d \quad [17]$$

where $\alpha = 10^{-3.46}$ and C_d is the concentration of deuteroyl ions in the porous-layer electrolyte at the b/p interface.

The first term on the right side of Eq. 15 is the Macdonald film-growth model (Eq. 49 of Ref 11). This is a model of film growth based on the diffusion of charged oxygen vacancies through the barrier layer from the m/b interface to the b/p interface. Mechanisms of chemical diffusion and electromigration are both included. The former results from a concentration gradient of vacancies within the film, the latter from the existence of an electric field within the film. It is assumed that the potential drop across the outer porous layer is negligible.

The second term on the right side of Eq. 15, which is fully defined in Eq. 16, is a rate law that is commonly used to describe the dissolution of a mineral into an aqueous medium.²¹ It actually is a simple way of describing the possibly complex processes that occur at the dissolving interface. The quantity j is known as the “order” of the reaction. Clearly, for dissolution to occur, we must have $C_z < C_{ze}$.

Equation 15 describes the combined processes of film growth taking place at the b/p interface and film reduction that occurs at the b/p interface. This general approach has been used in the past in the modeling of other oxidation-related phenomena, such as the kinetics of oxidation/volatilization by Tedmon²² and of oxidation/erosion by Markworth *et al.*²³

As far as the porous layer is concerned, let its thickness at time t be L_p . Its behavior in time is taken to be described quite simply by

$$\frac{dL_p}{dt} = R \quad [18]$$

In obtaining this expression, any difference in average density between the barrier and porous oxide is neglected. In addition, no account is taken of possible removal of porous-layer material, by whatever means, originating at the p/d interface, that is, the interface between the porous layer and the D_2O . Also, the structure (pore size, distribution, and interconnectivity) of the pores has not been included in the model at this stage and may be added during further refinement of the

model.

Next we describe the variation of C_d with respect to time, *i.e.*

$$\frac{dC_d}{dt} = \frac{k_2 A'(B-1)}{\exp(2KL_b) - 1} - k_3 R - \frac{k_4 D_d}{L_p} (C_d - C_{do}) \quad [19]$$

where k_2 , k_3 , and k_4 are new temperature-dependent rate parameters, D_d is the effective diffusivity of the deuteroyl ions through the porous-layer electrolyte, and C_{do} is the deuteroyl concentration in the electrolyte at the p/d interface. The first term on the right side of Eq. 19 is a statement of our assumption (see Eq. 14) that there is some deuteroyl generation in the porous layer at the b/p interface. This occurs at a rate proportional to the corrosion current, which in turn is proportional to the first term on the right side of Eq. 15. The proportionality factor, k_2 , is a function of several quantities, one of which is n in Eq. 14. The second term accounts for loss of deuteroyl at the b/p interface by reaction with ZrO_2 to form porous-layer material (see Eq. 11). The third term represents effective chemical diffusion of deuteroyl, through the electrolyte in the pores of the porous layer, from the b/p interface to the p/d interface. A linear concentration profile is assumed. This last term is based on an admittedly weak approximation. For example, we have not considered re-precipitation of zirconate ions, with consequent production of deuteroyl, which can occur to varying degrees throughout the volume the porous layer.

Finally, we express the temporal rate of change of C_z as

$$\frac{dC_z}{dt} = k_3 R - \frac{k_5 D_z}{L_p} (C_z - \alpha C_{do}) \quad [20]$$

where k_5 is still another temperature-dependent parameter and D_z is the effective chemical diffusivity of zirconate in the porous-layer electrolyte. The first term on the right side of Eq. 20 represents production of zirconate as porous-layer material is formed at the b/p interface. The second term represents effective chemical diffusion away from this interface through the porous-layer electrolyte. It is assumed that the zirconate and deuteroyl concentrations are in equilibrium at the p/d interface. Again, this second term does not include effects of zirconate reprecipitation with accompanying loss of this species from solution.

Equations 15-20 comprise a mathematical representation of the corrosion. They can be integrated numerically, provided that values for all the system parameters are known, which they most likely are not. However, this problem can at least be partially alleviated by expressing these equations in “universal” or dimensionless form. This has the advantage of removing all dependence on systems of units, it reduces the number of independent system parameters, and it facilitates any assessment of the relative importance of the various contributing mechanisms. Toward that end, we define the following dimensionless quantities

$$\tau = 2KA'(B-1)t \quad [21]$$

$$\lambda_b = 2KL_b, \quad \lambda_p = 2KL_p \quad [22]$$

$$\omega_{ze} = C_{ze}/C_{do}, \quad \omega_z = C_z/C_{do}, \quad \omega_d = C_d/C_{do} \quad [23]$$

$$\beta_1 = \frac{k_1(C_{do})^j}{A'(B-1)}, \quad \beta_2 = \frac{k_2}{2KC_{do}}, \quad \beta_3 = \frac{k_3(C_{do})^{j-1}}{2KA'(B-1)},$$

$$\beta_4 = \frac{k_4D_d}{A'(B-1)}, \quad \beta_5 = \frac{k_5D_z}{A'(B-1)} \quad [24]$$

and we note that $\omega_{ze} = \alpha\omega_d$. Combining these expressions with Eq. 15-20, we obtain the model as expressed in totally dimensionless form, *i.e.*

$$\frac{d\lambda_b}{d\tau} = \frac{1}{\exp(\lambda_b) - 1} - \beta_1(\alpha\omega_d - \omega_z)^j \quad [25]$$

$$\frac{d\lambda_p}{d\tau} = \beta_1(\alpha\omega_d - \omega_z)^j \quad [26]$$

$$\frac{d\omega_d}{d\tau} = \frac{\beta_2}{\exp(\lambda_b) - 1} - \beta_3(\alpha\omega_d - \omega_z)^j - \frac{\beta_4}{\lambda_p}(\omega_d - 1) \quad [27]$$

$$\frac{d\omega_z}{d\tau} = \beta_3(\alpha\omega_d - \omega_z)^j - \frac{\beta_5}{\lambda_p}(\omega_z - \alpha) \quad [28]$$

In this dimensionless form, the model has four independent variables and six independent system parameters (the five β 's and j). In its original form, there were 11 system parameters. The model is described in terms of four coupled, ordinary differential equations that are of first order and are nonlinear and autonomous.

*Sample calculations.—Introduction.—*We now present the results of numerically integrating Eq. 25-28 using selected sets of values for the β 's. In all these calculations, we assume first-order dissolution kinetics for the barrier layer, *i.e.*, $j = 1$, and we ignore diffusion of zirconate ions in the porous-layer electrolyte, *i.e.*, $\beta_5 = 0$. The numerical integration was carried out using a fourth-order Runge-Kutta method with fixed interval size. The software package Math-cad PLUS 5.0 was used to generate the solutions and plot the results.

It should be emphasized that we have explored the system's behavior only within a small portion of its parameter space. Nevertheless, the results we have obtained do have some features that are in qualitative agreement with experimental observations. It is entirely possible that the

most interesting and perhaps the most important behavior has not yet been seen. Because of its nonlinear character, the model can potentially exhibit a rich variety of behaviors, including spontaneous oscillations of system variables that are periodic, quasi-periodic, or even chaotic. Chaos is a possibility because the requirements of nonlinearity and at least three independent variables are both met. Bifurcations in dynamic behavior, as system parameters are varied, may also occur. Of course, such possibilities are only of academic interest if they occur only outside the operating conditions of interest.

The initial conditions we selected for integrating the dimension-less rate equations were that at $t = 0$, the four variables had the following values: $\lambda_b = 0.1$, $\lambda_p = 0.01$, $\omega_d = 1$, and $\omega_z = \alpha$. The slight initial offset from zero of λ_b and λ_p was done in order to keep the right sides of Eq. 25, 27, and 28 from diverging, which would have interfered with straightforward application of the Runge-Kutta method.

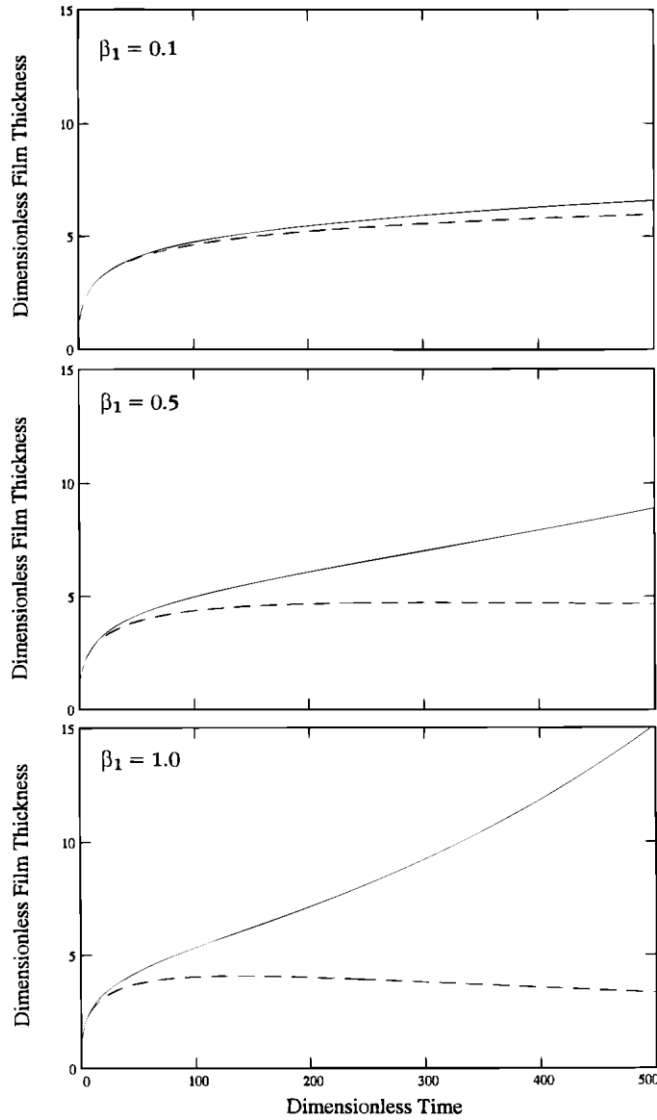


Figure 3. Film growth kinetics for β_1 as shown, $\beta_2 = 10$, $\beta_3 = 0.001$, $\beta_4 = 0.0001$.

Numerical results.—Figures 3-7 contain the results of numerically integrating the dimensionless rate equations (Eq. 25-28) for selected values of the rate parameters. It should be emphasized that the parameter values used in these calculations were not the result of any physically based reasoning. They were chosen simply because their use resulted in solutions that appeared to be “reasonable.” Beside that, our main interest at this point is just to obtain some qualitative assessment of how the predicted film-growth kinetics are affected as the various system parameters are varied, one at a time. It should be noted that in all five figures, the dashed curve represents the barrier film and the solid curve represents the total film, *i.e.*, barrier film plus porous layer.

The parameter β_1 can be seen from Eq. 25 and 26 to be one that plays a major role in development of the porous layer. An increase of β_1 essentially implies an increase in the rate at which barrier-layer material is changed to porous-layer material. Effects of varying this

parameter are shown in Fig. 3, wherein we find that an increase through an order of magnitude causes significant changes. The thickness of the barrier layer (at any given time) is suppressed, plus

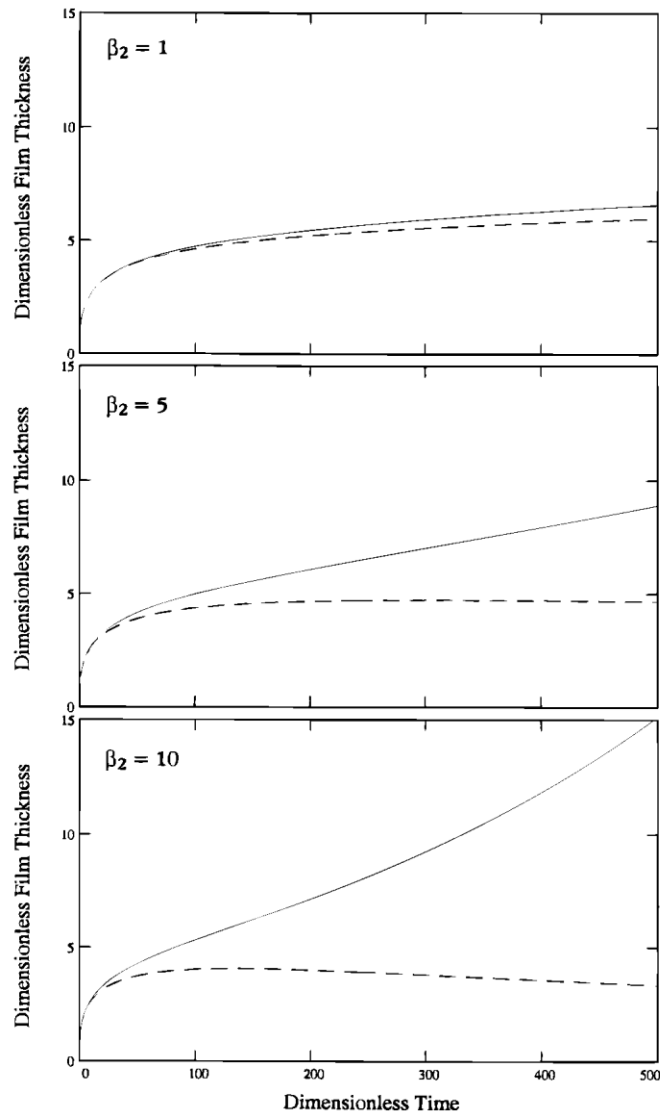


Figure 4. Film growth kinetics for $\beta_1 = 1$, β_2 as shown, $\beta_3 = 0.001$, $\beta_4 = 0.0001$.

the growth of the porous layer and of the total oxide thickness are considerably enhanced.

The parameter β_2 appears in Eq. 27 and is associated with the rate of deuteroyl production at the b/p interface. At least qualitatively, the effect of increasing β_2 , again through an order of magnitude, is seen in Fig. 4 to be quite similar to that of increasing β_1 , as shown in Fig. 3. From Eq. 27, we see that increasing β_2 causes the rate of deuteroyl production at the b/p interface to increase. This causes an increase of the equilibrium solubility of zirconate (after Eq. 17) and in turn, an increase of the rate of formation of the porous layer.

The parameter β_3 appears in Eq. 27 and 28 and is associated with loss of deuteroyl and with production of zirconate at the b/p interface. As illustrated in Fig. 5, increasing β_3 through two orders of magnitude causes some increase of barrier-layer thickness, substantial decrease of porous-layer thickness, and some thickness decrease for the entire oxide film. Decreasing the deuteroyl concentration and increasing the zirconate concentration both act to decrease R (after Eq. 16 and 17) and hence decrease the production rate of porous material.

The parameter β_4 is associated with chemical diffusion of deuteroyl through the porous-layer electrolyte, as seen in Eq. 27. Increasing this parameter can be regarded, among other things, as being equivalent to increasing the diffusivity, D_d , in the same proportion (see Eq.

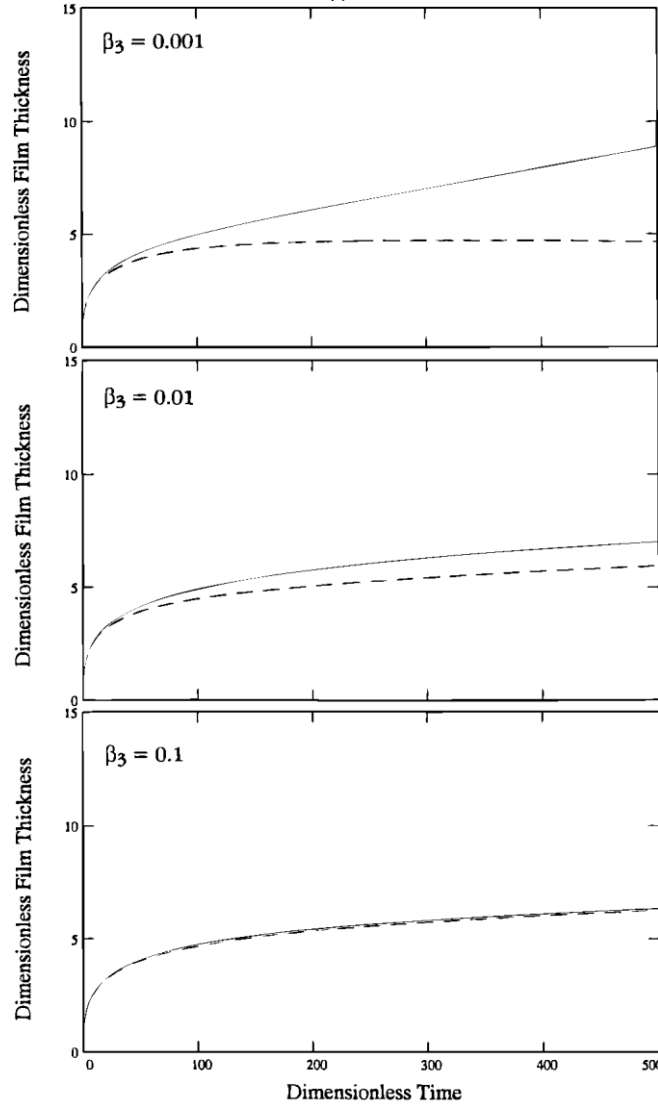


Figure 5. Film growth kinetics for $\beta_1 = 1$, $\beta_2 = 5$, β_3 as shown, $\beta_4 = 0.0001$.

24). Increasing the rate of transport of deuteroyl away from the b/p interface results in a decrease of the equilibrium zirconate concentration, and hence in a concomitant reduction of the rate of formation of porous material. Effects of an increase through an order of magnitude are shown in Fig. 6, the results of which are quite similar to those presented in Fig. 5 for increasing β_3 .

Finally, one of the calculations shown in Fig. 6 is repeated in Fig. 7, except that it is extended to a much larger time. At these larger times, the barrier layer is becoming slightly thinner, whereas the thickness of the entire film continues to increase, showing some upward curvature.

Conclusion

The increase in D content observed in some Zr-2.5 Nb pressure tubes after several years of use in CANDU reactors is unexplained. A model presented in the literature describes the corrosion rate of Zr-2.5 Nb pressure tubes to be constant and predicts a linear increase in D content.² This model is essentially a fit to the experimental data with little fundamental justification. It does not predict increases in corrosion rate that have been observed, and it cannot explain the high-D tubes.

In the present work, a new model for the D₂O-induced corrosion of zirconium pressure tubes is presented. The model describes the development of a two-layer oxide film consisting of a dense barrier layer in contact with the metal over which is a porous outer layer in

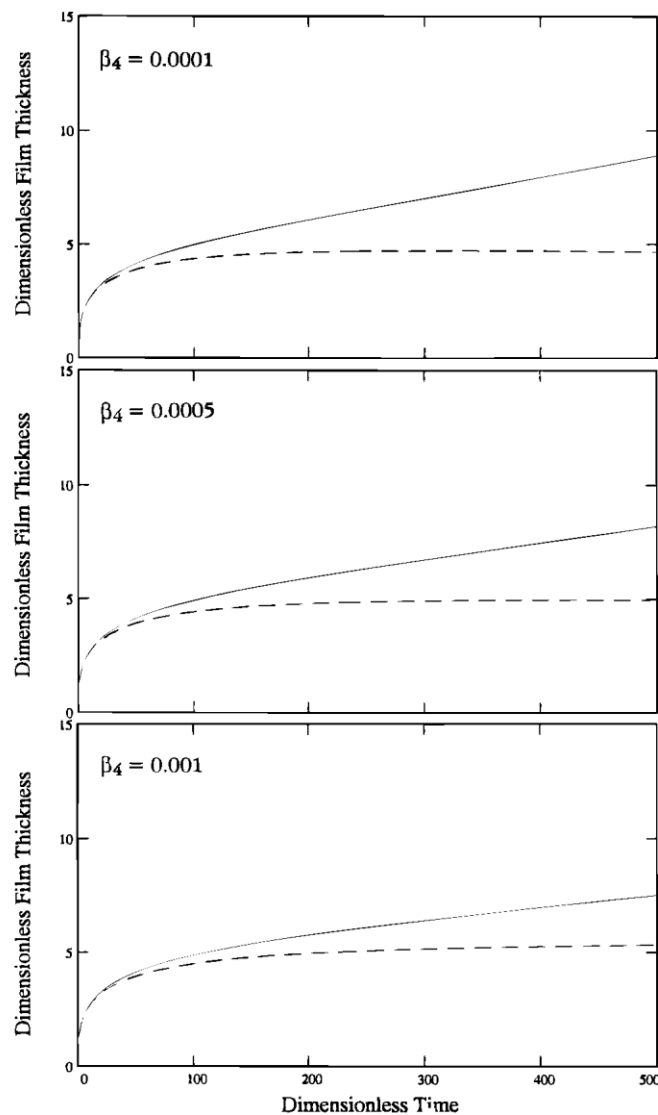


Figure 6. Film growth kinetics for $\beta_1 = 1$, $\beta_2 = 5$, $\beta_3 = 0.001$, β_4 as shown.

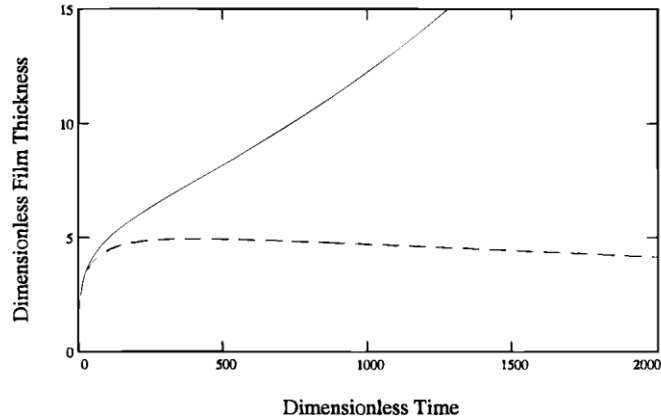


Figure 7. Film growth kinetics for $\beta_1 = 1$, $\beta_2 = 5$, $\beta_3 = 0.001$, $\beta_4 = 0.0005$ with τ taken to a value of 2000.

contact with the D_2O . Growth of the barrier layer is described using the film-growth model of Macdonald and co-workers.^{11,12,14,15} It is assumed that the porous layer develops as a result of the chemical dissolution of zirconia to form zirconate ions at the interface between the two layers.

Using somewhat arbitrarily selected values for the various rate parameters, we have numerically integrated the four coupled differential equations that describe the growth kinetics of the two films. General features of the calculated behavior are in agreement with observations of actual tubes. The barrier layer grows at an initially rapid rate and then reaches a saturation level (and may even shrink to a certain degree). The porous layer grows continuously and at a rate that varies widely with values chosen for the rate parameters.

Given its simplicity, it is encouraging that the model behaves as well as it does. Inclusion of other phenomena, such as reprecipitation of zirconate within the porous layer and removal of porous-layer material by some mechanism, would make the model more realistic. However, this would also add to its complexity as well as add new and possibly unknown rate parameters.

Acknowledgments

The authors thank A. Shalabi and G. Rzentkowski for providing key documents and for extensive discussions on the subject. Technical discussions with B. Warr, B. Cox, and V. Urbanic (as well as with several other AECL, Ontario Hydro, and Chalk River personnel) have also been extremely helpful and are greatly appreciated. Support of this work by the Atomic Energy Control Board under AECB project no. 2.349.1 is gratefully acknowledged.

The Ohio State University assisted in meeting the publication costs of this article.

List of Symbols

A	constant
A'	temperature-dependent parameter
B	temperature-dependent parameter
C_d	deuteroxyl ion concentration in the porous-layer electrolyte at the barrier/porous layer interface
C_{do}	deuteroxyl ion concentration in the porous-layer electrolyte at the porous/ D_2O solution layer interface
C_z	actual concentration of zirconate ions at the barrier/porous-layer interface
C_{ze}	equilibrium concentration of zirconate ions at the barrier/porous-layer electrolyte
D_{ab}	atomic deuterium absorbed on the oxide surface

D_{ad}	atomic deuterium adsorbed on the oxide surface
D_d	effective diffusivity of the deuteroyl ions through the porous-layer electrolyte
D_z	effective diffusivity of the zirconate ions through the porous-layer electrolyte
[D]	concentration of deuterium dissolved ion the Zr-2.5 Nb alloy
j	order of reaction
k	Boltzmann constant
k_i	temperature-dependent parameters with i varying from 1 to 5
K	temperature-dependent parameter
L_b	thickness of barrier layer at time t
L_p	thickness of porous layer at time t
n	fractional amount of reduction associated with deuteroyl formation
O_o	oxygen ion in the oxide layer sitting in an oxygen site
OD_{ad}^{n-}	charged deuteroyl species that is adsorbed on the barrier-layer/ porous-layer interface, n varies from 1 to 2
Q	activation energy required for deuterium diffusion through the barrier oxide layer
R	rate of change of the porous-layer thickness
t	time elapsed from start of exposure
T	absolute temperature (K)
V_O^{2+}	vacancy in the oxide where normally an oxygen ion would be present, has a 2+ charge due to lack of the 2-oxygen ion

Greek

α	$10^{-3.46}$
β_i	dimensionless temperature-dependent variable with i varying from 1 to 5
λ_b	dimensionless barrier-layer thickness
λ_p	dimensionless porous-layer thickness
ω_{ze}	dimensionless ratio of C_{ze} to C_{do}
ω_z	dimensionless ratio of C_z to C_{do}
ω_d	dimensionless ratio of C_d to C_o
τ	dimensionless time

References

1. M. B. Elmoselhi, B. D. Warr, and S. McIntyre, *Zirconium in Nuclear Industry: 10th International Symposium*, ASTM STP 1245, A. M. Garde and E. R. Bradley, Editors, p. 62, American Society for Testing and Materials, Philadelphia, PA (1994).
2. B. D. Warr, N. Ramasubramanian, M. B. Elmoselhi, F. R. Greening, Y-P. Lin, and P. C. Lichtenberger, *Ontario Hydro Research Review No. 8* (Aug 1993).
3. B. D. Warr, M. B. Elmoselhi, S. B. Newcomb, N. S. McIntyre, A. M. Brennenstuhl, and P. C. Lichtenberger, *Zirconium in the Nuclear Industry: 9th International Symposium*, ASTM STP 1132, C. M. Eucken and A. M. Garde, Editors, p. 740, American Society for Testing and Materials, Philadelphia, PA (1991).
4. IAEA-TECDOC-996 (Jan 1998).
5. E. G. Price, AECL Report-8338 (Oct 1984).
6. D. D. Lanning, A. B. Johnson, Jr., D. J. Trimble, and S. M. Boyd, *Zirconium in the Nuclear Industry: 8th International Symposium*, ASTM STP 1023, L. F. P. Van Swam and C. M. Eucken, Editors, p. 3, American Society for Testing and Materials, Philadelphia, PA (1989).
7. V. F. Urbanic, B. D. warr, A. Manolescu, C. K. Chow, and M. W. Shanahan, *Zirconium in the Nuclear Industry: 8th International Symposium*, ASTM STP 1023, L. F. P. Van Swam and C. M. Eucken, Editors, p. 20, American Society for Testing and Materials, Philadelphia, PA (1989).
8. B. D. Warr, P. A. W. Vam Der Heidi, and M. A. Maguire, *Zirconium in the Nuclear Industry: 11th International Symposium*, ASTM STP 1295, E. R. Bradley and G. P. Sabol, Editors, p. 265, American Society for Testing and Materials, Philadelphia, PA (1996).
9. D. O. Northwood and U. Kosasih, *Inter. Metals Review*, Vol. 28, No. 2, p. 92, 1983, and references therein.
10. E. Hillner, WPAD-TM-411 (Nov 1964).
11. C. Y. Chao, L. F. Lin, and D. D. Macdonald, *J. Electrochem. Soc.*, **128**, 1187 (1981).
12. L. F. Lin, C. Y. Chao, and D. D. Macdonald, *J. Electrochem. Soc.*, **128**, 1194 (1981).
13. B. Cox and C. Roy, AECL Report-2519 (Dec 1965).

14. D. D. Macdonald, *J. Electrochem. Soc.*, **139**, 3434 (1992) and references therein.
15. L. Zhang, D. D. Macdonald, E. Sikora, and J. Sikora, *J. Electrochem. Soc.*, **145**, 898 (1998).
16. D. D. Macdonald, International Hard Anodizing Meeting, San Diego, CA (Oct 1998).
17. O. Pensado-Rodriguez, M. Urquidi-Macdonald, J. R. Flores, and D. D. Macdonald, *Passivity and Its Breakdown*, P. M. Natishan, H. S. Isaacs, M. Janik-Czachor, V. A. Macagno, P. Marcus, and M. Seo, Editors, PV 97-26, p. 870, The Electrochemical Society Proceedings Series, Pennington, NJ (1997).
18. O. Pensado-Rodriguez, M. Urquidi-Macdonald, and J. R. Flores, Abstract 1070, The Electrochemical Society Meeting Abstracts, Vol. 98-2, Boston, MA, Nov 1-6, 1998.
19. M. Pourbaix, *Atlas of Electrochemical Equilibria in Aqueous Solutions*, NACE, Houston, TX (1974).
20. B. Cox and V. Fidleris, *Zirconium in Nuclear Industry: 8th International Symposium*, ASTM STP 1023, L. F. P. Van Swam and C. M. Eucken, Editors, p. 245, American Society for Testing and Materials, Philadelphia, PA (1989).
21. A. C. Lasaga, in *Kinetics of Geochemical Processes, Rev. Minerology*, Vol. 8, A. C. Lasaga and R. J. Kirkpatrick, Editors, p. 1, The Minerology Society of America, Washington, DC (1981).
22. C. S. Tedmon, Jr., *J. Electrochem. Soc.*, **113**, 766 (1966).
23. A. J. Markworth, V. Nagarajan, and I. G. Wright, *Oxid. Met.*, **35**, 89 (1991).